

# Exact results for quench dynamics and defect production in a two-dimensional model

K. Sengupta<sup>1</sup>, Diptiman Sen<sup>2</sup> and Shreyoshi Mondal<sup>1</sup>

<sup>1</sup> *TCMP division, Saha Institute of Nuclear Physics, 1/AF Bidhannagar, Kolkata 700 064, India*

<sup>2</sup> *Center for High Energy Physics, Indian Institute of Science, Bangalore, 560 012, India*

(Dated: October 29, 2018)

We show that for a  $d$ -dimensional model in which a quench with a rate  $\tau^{-1}$  takes the system across a  $d - m$  dimensional critical surface, the defect density scales as  $n \sim 1/\tau^{m\nu/(z\nu+1)}$ , where  $\nu$  and  $z$  are the correlation length and dynamical critical exponents characterizing the critical surface. We explicitly demonstrate that the Kitaev model provides an example of such a scaling with  $d = 2$  and  $m = \nu = z = 1$ . We also provide the first example of an exact calculation of some multispin correlation functions for a two-dimensional model which can be used to determine the correlation between the defects. We suggest possible experiments to test our theory.

PACS numbers: 73.43.Nq, 05.70.Jk, 64.60.Ht, 75.10.Jm

Quantum phase transitions have been studied extensively for several years [1]. Such a transition is accompanied by diverging length and time scales [1] leading to the absence of adiabaticity close to the quantum critical point. Thus the system fails to follow its instantaneous ground state when some parameter in its Hamiltonian is varied in time at a finite rate  $1/\tau$  which takes the system across the critical point. Since the final state of the system does not conform to the ground state of its final Hamiltonian, defects are produced [2, 3]. The defect density  $n$  depends on the quench time  $\tau$  as  $n \sim 1/\tau^{d\nu/(\nu z+1)}$ , where  $\nu$  and  $z$  are the correlation length and dynamical critical exponents at the critical point [4]. A theoretical study of such a quench dynamics requires a knowledge of the excited states of the system. Such studies have therefore been mostly restricted to phase transitions in exactly solvable models in one or infinite dimensions [5, 6, 7, 8]. Experimental studies of defect production due to quenching of the magnetic field in a two-dimensional (2D) spin-1 Bose condensate have been undertaken [9]. However, exact studies of quench dynamics have not been carried out so far for 2D spin models.

In this Letter, we carry out such a study for the 2D Kitaev model [10]. We show that when the quench takes the system across a critical (gapless) line, the density of defects scales as  $1/\sqrt{\tau}$ . The Kitaev model has  $d = 2$  and  $\nu = z = 1$ ; hence, the above scaling is in contrast to the  $n \sim 1/\tau$  behavior expected when the system passes through a critical point [4]. In this context we provide a general discussion of the scaling of the defect density for a general  $d$ -dimensional model with arbitrary  $\nu$  and  $z$ ; we show that when the quench takes such a system through a  $d - m$  dimensional gapless (critical) surface, the defect density scales as  $n \sim 1/\tau^{m\nu/(z\nu+1)}$ . This result is a generalization of the result of Ref. [4] and hence constitutes a significant extension of our current understanding of defect production due to a quench. We also compute exactly some multispin correlation functions for our model, and use them to study the variation of defect correlations with the quench rate and the model param-

eters. Such an exact analysis of defect correlations has not been carried out so far for 2D systems.

The Kitaev model is a spin-1/2 model on a 2D honeycomb lattice with the Hamiltonian [10]

$$H = \sum_{j+l=\text{even}} (J_1 \sigma_{j,l}^x \sigma_{j+1,l}^x + J_2 \sigma_{j-1,l}^y \sigma_{j,l}^y + J_3 \sigma_{j,l}^z \sigma_{j,l+1}^z), \quad (1)$$

where  $j$  and  $l$  denote the column and row indices of the lattice. This model, sketched in Fig. 1, is known to have several interesting features [12, 13, 14, 15]. It is a rare example of a 2D model which can be exactly solved [10, 12, 14]. It supports a gapless phase for  $|J_1 - J_2| \leq J_3 \leq J_1 + J_2$  [10] which is possibly connected to a spin liquid state and demonstrates fermion fractionalization at all energy scales [13]. In certain parameter regimes, the ground state exhibits topological order and the low-energy excitations carry Abelian and non-Abelian fractional statistics; these excitations can be viewed as robust qubits in a quantum computer [11]. There have been proposals for experimentally realizing this model in systems of ultracold atoms and molecules trapped in optical lattices [16]; such systems are known to provide easy access to the study of non-equilibrium dynamics of the underlying model. However, in spite of several studies of the phases and low-lying excitations of the Kitaev model, its non-equilibrium dynamics has not been studied so far. We will study what happens in this model when  $J_3$  is varied from  $-\infty$  to  $\infty$  at a rate  $1/\tau$ , keeping  $J_1$  and  $J_2$  fixed.

One of the main properties of the Kitaev model which makes it theoretically attractive is that, even in 2D, it can be mapped onto a non-interacting fermionic model by a suitable Jordan-Wigner transformation [12, 14],

$$H_F = i \sum_{\vec{n}} [J_1 b_{\vec{n}} a_{\vec{n}-\vec{M}_1} + J_2 b_{\vec{n}} a_{\vec{n}+\vec{M}_2} + J_3 D_{\vec{n}} b_{\vec{n}} a_{\vec{n}}], \quad (2)$$

where  $a_{\vec{n}}$  and  $b_{\vec{n}}$  are Majorana fermions sitting at the top and bottom sites respectively of a bond labeled  $\vec{n}$ ,  $\vec{n} = \sqrt{3}\hat{i} n_1 + (\frac{\sqrt{3}}{2}\hat{i} + \frac{3}{2}\hat{j}) n_2$  denote the midpoints of the

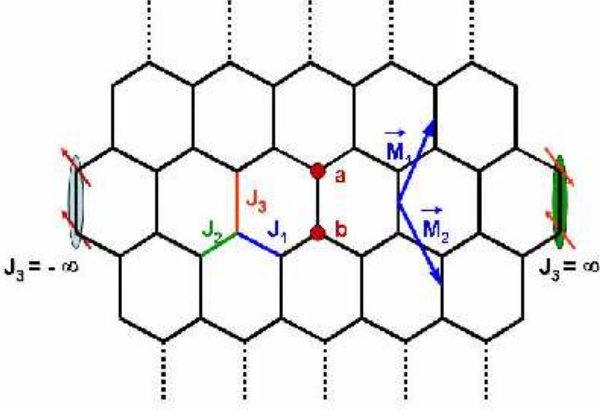


FIG. 1: Schematic representation of the Kitaev model on a honeycomb lattice showing the bonds  $J_1$ ,  $J_2$  and  $J_3$ . Schematic pictures of the ground states, which correspond to pairs of spins on vertical bonds locked parallel (antiparallel) to each other in the limit of large negative (positive)  $J_3$ , are shown at one bond on the left (right) edge respectively.  $\vec{M}_1$  and  $\vec{M}_2$  are spanning vectors of the lattice, and  $a$  and  $b$  represent inequivalent sites.

vertical bonds shown in Fig. 1, and  $n_1, n_2$  run over all integers. The vectors  $\vec{n}$  form a triangular lattice. The  $x, y$  coordinates of the triangular lattice sites are given by  $x = \sqrt{3}(n_1 + n_2/2)$  and  $y = 3n_2/2$ . [We will refer to the sites of the honeycomb lattice either as  $(j, l)$  as in Eq. (1), or as  $(a, \vec{n})$  and  $(b, \vec{n})$  as in Eq. (2);  $j + l$  is even (odd) for  $a$  ( $b$ ) sites respectively.] The vectors  $\vec{M}_1 = \frac{\sqrt{3}}{2}\hat{i} + \frac{3}{2}\hat{j}$  and  $\vec{M}_2 = \frac{\sqrt{3}}{2}\hat{i} - \frac{3}{2}\hat{j}$  are spanning vectors for the reciprocal lattice. The operator  $D_{\vec{n}}$  can take the values  $\pm 1$  independently for each  $\vec{n}$  and commutes with  $H_F$ , so that the states can be labeled by the values of  $D_{\vec{n}}$  on each bond; the ground state corresponds to  $D_{\vec{n}} = 1$  on all bonds [10, 12, 13, 14] irrespective of the sign of  $J_3$  due to a special symmetry of the model [10]. Since  $D_{\vec{n}}$  is a constant of motion, the dynamics of the model starting from the ground state never takes the system outside the manifold of states with  $D_{\vec{n}} = 1$ .

For  $D_{\vec{n}} = 1$ , Eq. (2) can be diagonalized as  $H_F = \sum_{\vec{k}} \psi_{\vec{k}}^\dagger H_{\vec{k}} \psi_{\vec{k}}$ , where  $\psi_{\vec{k}}^\dagger = (a_{\vec{k}}^\dagger, b_{\vec{k}}^\dagger)$  are Fourier transforms of  $a_{\vec{n}}$  and  $b_{\vec{n}}$ , the sum over  $\vec{k}$  extends over half the Brillouin zone (BZ) of the triangular lattice formed by the vectors  $\vec{n}$ , and  $H_{\vec{k}}$  can be expressed in terms of the Pauli matrices  $\sigma^i$  (where  $\sigma^3$  is diagonal) as  $H_{\vec{k}} = 2[J_1 \sin(\vec{k} \cdot \vec{M}_1) - J_2 \sin(\vec{k} \cdot \vec{M}_2)]\sigma^1 + 2[J_3 + J_1 \cos(\vec{k} \cdot \vec{M}_1) + J_2 \cos(\vec{k} \cdot \vec{M}_2)]\sigma^2$ . The spectrum consists of two bands with energies  $E_{\vec{k}}^\pm = \pm E_{\vec{k}}$ , where

$$E_{\vec{k}} = 2\{[J_1 \sin(\vec{k} \cdot \vec{M}_1) - J_2 \sin(\vec{k} \cdot \vec{M}_2)]^2 + [J_3 + J_1 \cos(\vec{k} \cdot \vec{M}_1) + J_2 \cos(\vec{k} \cdot \vec{M}_2)]^2\}^{1/2} \quad (3)$$

For  $|J_1 - J_2| \leq J_3 \leq J_1 + J_2$ , the bands touch each other, and the energy gap  $\Delta_{\vec{k}} = E_{\vec{k}}^+ - E_{\vec{k}}^-$  vanishes for special

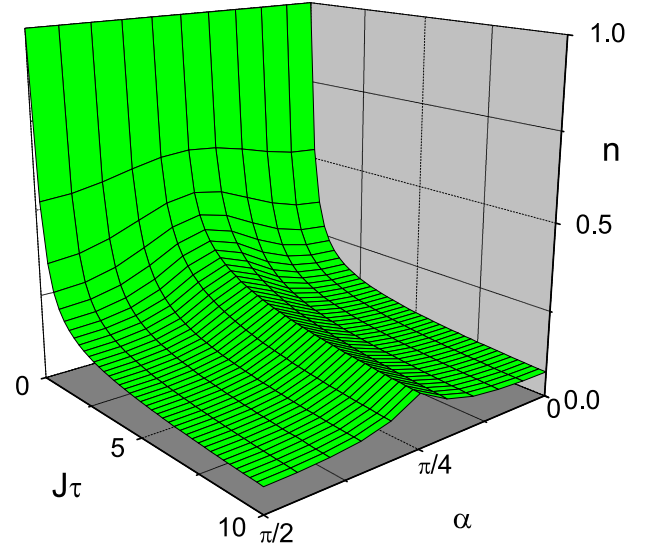


FIG. 2: Plot of defect density  $n$  versus  $J\tau$  and  $\alpha = \tan^{-1}(J_2/J_1)$ . The density of defects is maximum at  $J_1 = J_2$ .

values of  $\vec{k}$  leading to a gapless phase [10, 12, 14, 15].

We will now quench  $J_3(t) = Jt/\tau$  from  $-\infty$  to  $\infty$  at a fixed rate  $1/\tau$ , keeping  $J$ ,  $J_1$  and  $J_2$  fixed at some positive values. The ground states of  $H_F$  corresponding to  $J_3 \rightarrow -\infty(\infty)$ , schematically shown in Fig. 1, are gapped and have  $\sigma_{j,l}^z \sigma_{j,l+1}^z = 1(-1)$  for all lattice sites  $(j, l)$  of type  $b$ . To study the time evolution of the system, we note that after an unitary transformation  $U = \exp(-i\sigma^1\pi/4)$ , we obtain  $H_F = \sum_{\vec{k}} \psi_{\vec{k}}^\dagger H_{\vec{k}}' \psi_{\vec{k}}'$ , where  $H_{\vec{k}}' = UH_{\vec{k}}U^\dagger$  is given by  $H_{\vec{k}}' = 2[J_1 \sin(\vec{k} \cdot \vec{M}_1) - J_2 \sin(\vec{k} \cdot \vec{M}_2)]\sigma^1 + 2[J_3(t) + J_1 \cos(\vec{k} \cdot \vec{M}_1) + J_2 \cos(\vec{k} \cdot \vec{M}_2)]\sigma^3$ . Hence the off-diagonal elements of  $H_{\vec{k}}'$  remain time independent, and the quench dynamics reduces to a Landau-Zener problem for each  $\vec{k}$ . The defect density can then be computed following a standard prescription [17]:  $n = (1/A) \int_{\vec{k}} d^2\vec{k} p_{\vec{k}}$ , where

$$p_{\vec{k}} = \exp[-2\pi\tau\{J_1 \sin(\vec{k} \cdot \vec{M}_1) - J_2 \sin(\vec{k} \cdot \vec{M}_2)\}^2/J] \quad (4)$$

is the probability of defect production for the state labeled by momentum  $\vec{k}$ , and  $A = 4\pi^2/(3\sqrt{3})$  denotes the area of half the BZ over which the integration is carried out. A plot of  $n$  as a function of the quench time  $J\tau$  and an angle  $\alpha$  is shown in Fig. 2; here we have taken  $J_{1[2]} = J \cos \alpha[\sin \alpha]$ . We note that the density of defects produced is maximum when  $\alpha = \pi/4$  ( $J_1 = J_2$ ). This occurs because the length of the gapless line through which the system passes during the quench is maximum for  $J_1 = J_2$ . Hence the system remains in the non-adiabatic state for the maximum time during the quench, leading to the maximum density of defects. Note that unlike some other models [5], the defects here do not correspond to topological defects since the dynamics always keeps  $D_{\vec{n}} = 1$  on all bonds.

For sufficiently slow quench  $2\pi J\tau \gg 1$ ,  $p_{\vec{k}}$  is exponentially small for all values of  $\vec{k}$  except near the line  $J_1 \sin(\vec{k} \cdot \vec{M}_1) = J_2 \sin(\vec{k} \cdot \vec{M}_2)$ ; the contribution to the momentum integral in the expression for  $n$  comes from this region. Note that the line  $p_{\vec{k}} = 1$  precisely corresponds to the zeros of the energy gap  $\Delta_{\vec{k}}$  as  $J_3$  is varied for fixed  $J_1, J_2$ . By expanding  $p_{\vec{k}}$  about this line, we see that for a very slow quench, the defect density scales as  $n \sim 1/\sqrt{\tau}$ . This demonstrates that the scaling of  $n$  with  $\tau$  crucially depends on the dimensionality of the critical surface since for a quench which takes the system through a *critical point* instead of a *critical line*, the defect density of the Kitaev model, which has  $d = 2$  and  $\nu = z = 1$  [18], is expected to scale as  $1/\tau$  [4]. This observation leads to the following general conclusion.

Consider a  $d$ -dimensional model with  $\nu = z = 1$  which is described by a Hamiltonian  $H_d = \sum_{\vec{k}} \psi_{\vec{k}}^\dagger \left( \sigma^3 \epsilon(\vec{k}) t/\tau + \Delta(\vec{k}) \sigma^+ + \Delta^*(\vec{k}) \sigma^- \right) \psi_{\vec{k}}$ , where  $\sigma^\pm = (\sigma^1 \pm i\sigma^2)/2$ . Suppose that a quench takes the system through a critical surface of  $d - m$  dimensions. The defect density for a sufficiently slow quench is given by [17]  $n = (1/A_d) \int_{\text{BZ}} d^d k e^{-\pi\tau f(\vec{k})} \simeq (1/A_d) \int_{\text{BZ}} d^d k \exp[-\pi\tau \sum_{\alpha,\beta=1}^m g_{\alpha\beta} k_\alpha k_\beta] \sim 1/\tau^{m/2}$ , where  $A_d$  is the area of the  $d$ -dimensional BZ,  $f(\vec{k}) = |\Delta(\vec{k})|^2/|\epsilon(\vec{k})|$  vanishes on the  $d - m$  dimensional critical surface,  $\alpha, \beta$  denote one of the  $m$  directions orthogonal to that surface, and  $g_{\alpha\beta} = [\partial^2 f(\vec{k})/\partial k_\alpha \partial k_\beta]_{\vec{k} \in \text{critical surface}}$ . Note that this result depends only on the property that  $f(\vec{k})$  vanishes on a  $d - m$  dimensional surface, and not on the precise form of  $f(\vec{k})$ . For general values of  $\nu$  and  $z$ , we note that a Landau-Zener type of scaling argument yields  $\Delta \sim 1/\tau^{z\nu/(z\nu+1)}$ , where  $\Delta$  is the energy gap [4]. When one crosses a  $d - m$  dimensional critical surface during the quench, the available phase space  $\Omega$  for defect production scales as  $\Omega \sim k^m \sim \Delta^{m/z} \sim 1/\tau^{m\nu/(z\nu+1)}$ ; this leads to  $n \sim 1/\tau^{m\nu/(z\nu+1)}$ . For a quench through a critical point where  $m = d$ , we retrieve the results of Ref. [4].

Next we study the correlations between the defects produced during the quench. To this end, we define the operators  $O_{\vec{r}} = ib_{\vec{n}} a_{\vec{n}+\vec{r}}$ . In the spin language,  $O_{\vec{0}} = \sigma_{j,l}^z \sigma_{j',l+1}^z$ . For  $\vec{r} \neq \vec{0}$ ,  $O_{\vec{r}}$  can be written as a product of spin operators going from a  $b$  site at  $\vec{n}$  to an  $a$  site at  $\vec{n} + \vec{r}$ : the product begins with a  $\sigma^x$  or  $\sigma^y$  at  $(j, l)$  and ends with a  $\sigma^x$  or  $\sigma^y$  at  $(j', l')$  with a string of  $\sigma^z$ 's in between, where the forms of the initial and final  $\sigma$  matrices depend on the positions of  $j + l$  and  $j' + l'$ . Note that for  $J_3 \rightarrow -\infty(\infty)$ , where the  $z$  component of each spin is locked with that of its vertically nearest neighbor,  $\langle \psi_{-\infty(\infty)} | O_{\vec{r}} | \psi_{-\infty(\infty)} \rangle = \pm \delta_{\vec{r}, \vec{0}}$ . For the Kitaev model, it is known that the spin correlations between sites lying on different bonds vanish, *e.g.*,  $\langle \sigma_{a,\vec{n}}^z \sigma_{b,\vec{n}+\vec{r}}^z \rangle = 0$  for  $\vec{r} \neq \vec{0}$  [13]. Therefore  $\langle O_{\vec{r}} \rangle$  are the only non-vanishing two-point correlators of the model [14]. A non-zero value of  $\langle O_{\vec{r}} \rangle$  for  $\vec{r} \neq \vec{0}$  in the final state provides a signature of

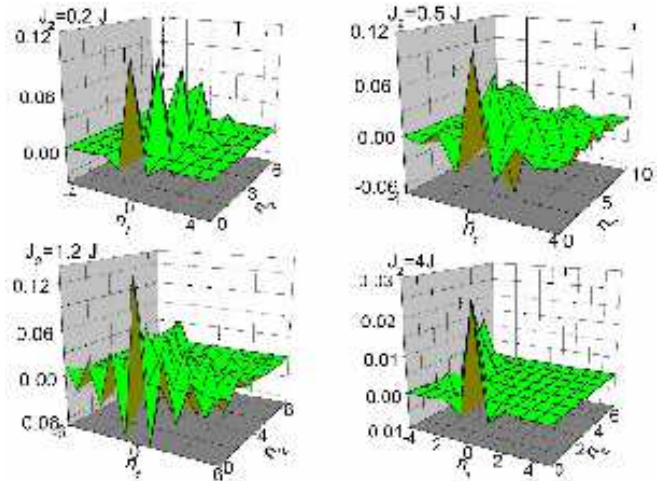


FIG. 3: Plot of  $\langle O_{\vec{r}} \rangle$ , sans the  $\delta$ -function peak at the origin, as a function of  $\vec{r}$  for four values of  $J_2/J_1$ , for  $J\tau = 5$ .

the defects. In particular, a plot of  $\langle O_{\vec{r}} \rangle$  versus  $\vec{r}$  gives an estimate of the correlations between the defects. [Since  $O_{\vec{r}}^2 = 1$ , all the moments of  $O_{\vec{r}}$  can be found trivially:  $\langle O_{\vec{r}}^n \rangle = \langle O_{\vec{r}} \rangle$  if  $n$  is odd and  $= 1$  if  $n$  is even.]

After the quench, the system, for each momentum  $\vec{k}$ , is described by a combination of  $\psi_{-\infty\vec{k}}$  with probability  $p_{\vec{k}}$  and  $\psi_{\infty\vec{k}}$  with probability  $1 - p_{\vec{k}}$ , where  $\psi_{\pm\infty\vec{k}}$  are the eigenstates of  $H_{\vec{k}}$  for  $J_3 \rightarrow \pm\infty$ . Hence  $\langle O_{\vec{r}} \rangle$  can be computed in a straightforward manner:

$$\langle O_{\vec{r}} \rangle = -\delta_{\vec{r}, \vec{0}} + \frac{2}{A} \int d^2\vec{k} p_{\vec{k}} \cos(\vec{k} \cdot \vec{r}), \quad (5)$$

where the integral runs over half the BZ with area  $A$ .

For large values of  $\tau$ , the dominant contribution comes from the region near the line  $J_1 \sin(\vec{k} \cdot \vec{M}_1) = J_2 \sin(\vec{k} \cdot \vec{M}_2)$  where  $p_{\vec{k}} = 1$ . Introducing the variables  $k_{\parallel}$  and  $k_{\perp}$  which vary along and perpendicular to this line (along the directions  $\hat{n}_{\parallel}$  and  $\hat{n}_{\perp}$  respectively), we see that the integrand in Eq. (5) takes the form  $\exp[-a(\vec{k}_0)\tau k_{\perp}^2 \pm i(\vec{k}_0 + k_{\parallel}\hat{n}_{\parallel} + k_{\perp}\hat{n}_{\perp}) \cdot \vec{r}]$ , where  $a(\vec{k}_0)$  is a number depending on  $\vec{k}_0$ . The evaluation of the integral over  $k_{\perp}$  gives a factor of  $\exp[-(\vec{r} \cdot \hat{n}_{\perp})^2/(4a\tau)]/\sqrt{a\tau}$ . We thus see that the magnitude of the defect correlations goes as  $1/\sqrt{\tau}$ , while the spatial extent of the correlations goes as  $\sqrt{\tau}$ . This is confirmed by the following relation:  $\sum_{\vec{r}} \vec{r}^2 \langle O_{\vec{r}} \rangle = -2(\nabla_{\vec{k}}^2 p_{\vec{k}})_{\vec{k}=\vec{0}} = 24\pi\tau(J_1^2 + J_2^2 + J_1J_2)/J$ .

To study the correlations between defects, we evaluate Eq. (5) numerically; the  $\vec{r}$  dependence of  $\langle O_{\vec{r}} \rangle$  is shown in Fig. 3 for several values of  $J_2/J_1$ , where  $J_1 = J$  and  $J\tau = 5$ . Here we have omitted the  $\delta$ -function peak at  $\vec{r} = \vec{0}$  in Eq. 5 so as to make the correlation at  $\vec{r} \neq \vec{0}$  clearly visible. The plot of  $\langle O_{\vec{r}} \rangle$  reflects the defect correlations. To understand the variation of these correlations with the ratio  $J_2/J_1$ , we note that for large  $J\tau$ , the maximum contribution to  $\langle O_{\vec{r}} \rangle$  comes from around the wave

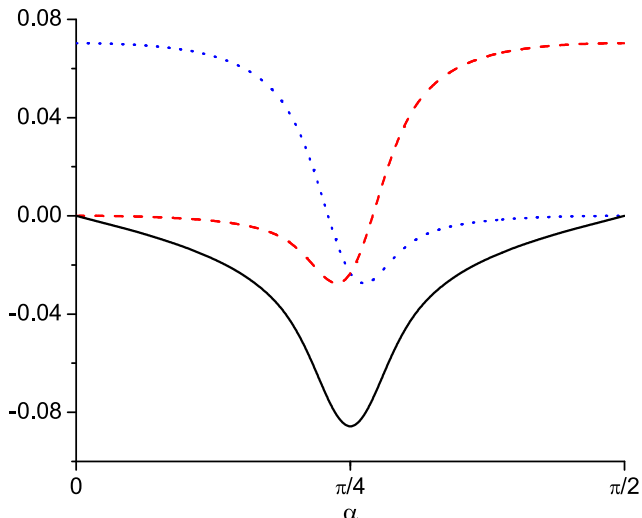


FIG. 4: Plot of  $\langle O_{\vec{r}} \rangle$  at the points  $(1, 0)$  on the  $n_1$  axis (black solid line),  $(0, 2)$  on the  $n_2$  axis (blue dotted line), and  $(2, -2)$  along the  $-45^\circ$  line in the  $n_1 - n_2$  plane (red dashed line) as a function of  $\alpha = \tan^{-1}(J_2/J_1)$ , for  $J^2 = 1$  and  $J\tau = 5$ .

vectors  $\vec{k}_0$  for which  $p(\vec{k}_0) = 1$ . For  $J_2 \gg (\ll) J_1$ , this implies  $\sin[\vec{k} \cdot \vec{M}_2(\vec{M}_1)] = 0$  which yields  $\vec{k}_0 \sim \sqrt{3}\hat{i} \pm \hat{j}$ . The maximum contribution to  $\langle O_{\vec{r}} \rangle$  comes from  $\cos(\vec{k}_0 \cdot \vec{r}) = 1$ , i.e.,  $\vec{k}_0 \cdot \vec{r} = 0$ . Thus for  $J_2 \gg (\ll) J_1$ ,  $\langle O_{\vec{r}} \rangle$  is expected to be maximal along the lines  $y = -(+)\sqrt{3}x$ , namely,  $n_1 = -n_2$  ( $n_1 = 0$ ) in the  $n_1 - n_2$  plane. This expectation is confirmed in Fig. 3 where  $\langle O_{\vec{r}} \rangle$  can be seen to be maximal along  $n_1 = -n_2$  ( $n_1 = 0$ ) for  $J_2 = 4(0.2)J_1$ . Such a strong anisotropy can be understood by noting that the Kitaev model reduces to a one-dimensional model when  $J_2 \gg (\ll) J_1$ . For intermediate values of  $J_1/J_2$ , a gradual evolution of the defect correlations can be seen in Fig. 3. We note that if the Kitaev model can be realized using ultracold atoms in an optical lattice [16], such an evolution of the defect correlations with  $J_1/J_2$  can, in principle, be experimentally detected by spatial noise correlation measurements as pointed out in Ref. [19].

We can obtain a different view of the spatial anisotropy of the defect correlations by studying  $\langle O_{\vec{r}} \rangle$  as a function of  $\alpha = \tan^{-1}(J_2/J_1)$ . As  $\alpha$  changes, the ratio  $J_2/J_1$  varies from 0 to  $\infty$  while fixing  $J_1^2 + J_2^2 = J^2 = 1$ . A plot of  $\langle O_{\vec{r}} \rangle$  at three representative points  $(n_1, n_2) = (1, 0)$  (on the  $n_1$  axis),  $(0, 2)$  (on the  $n_2$  axis), and  $(2, -2)$  (along the  $-45^\circ$  line in the  $n_1 - n_2$  plane) as a function of  $\alpha$ , shown in Fig. 4, reveals the nature of the defect correlations. We see that as  $J_2/J_1 = \tan \alpha$  is varied from 0 to  $\infty$ , the magnitude of the correlation at the point  $(1, 0)$  on the  $n_1$  axis increases till it reaches a maximum at  $J_1 = J_2$  ( $\alpha = \pi/4$ ), and then decays to 0 as  $\alpha$  approaches  $\pi/2$ . For the points  $(0, 2)$  on the  $n_2$  axis and  $(2, -2)$  along the line with slope  $-45^\circ$ , the correlation becomes maximum when  $J_2 \ll J_1$  ( $\alpha = 0$ ) and  $J_2 \gg J_1$  ( $\alpha = \pi/2$ ) respectively,

as expected from Fig. 3. We conclude that the spatial anisotropy of the correlations between the defects  $\langle O_{\vec{r}} \rangle$  depends crucially on the ratio  $J_2/J_1$ .

To conclude, we have shown that the density of defects produced during a quench of the Kitaev model through a critical line scales with the quench time as  $1/\sqrt{\tau}$ , instead of the  $1/\tau$  behavior expected for a quench through a critical point. We have provided a general result for the defect density which reproduces the result of Ref. [4] as a special case. We have also discussed the variation of the defect correlations with the model parameters and pointed out the possibility of detection of these variations in experiments. These results significantly improve our general understanding of the scaling of the density of defects and their correlations in 2D systems.

We thank A. Dutta and A. Polkovnikov for stimulating discussions.

- 
- [1] S. Sachdev, *Quantum Phase Transitions* (Cambridge University Press, Cambridge, England, 1999).
  - [2] T. W. B. Kibble, *J. Phys. A* **9**, 1387 (1976); W. H. Zurek, *Nature (London)* **317**, 505 (1985).
  - [3] B. Damski, *Phys. Rev. Lett.* **95**, 035701 (2005).
  - [4] A. Polkovnikov, *Phys. Rev. B* **72**, 161201(R) (2005); A. Polkovnikov and V. Gritsev, arXiv:0706.0212.
  - [5] K. Sengupta, S. Powell, and S. Sachdev *Phys. Rev. A* **69**, 053616 (2004); P. Calabrese and J. Cardy, *J. Stat. Mech: Theory Expt* P04010 (2005), and *Phys. Rev. Lett.* **96**, 136801 (2006); J. Dziarmaga, *Phys. Rev. Lett.* **95**, 245701 (2005), and *Phys. Rev. B* **74**, 064416 (2006).
  - [6] A. Das *et al.*, *Phys. Rev. B* **74**, 144423 (2006).
  - [7] R. W. Cherng and L. S. Levitov, *Phys. Rev. A* **73**, 043614 (2006); V. Mukherjee *et al.*, *Phys. Rev. B* **76**, 174303 (2007).
  - [8] B. Damski and W. H. Zurek, *Phys. Rev. A* **73**, 063405 (2006); F. M. Cucchietti *et al.*, *Phys. Rev. A* **75**, 023603 (2007); T. Caneva, R. Fazio, and G. E. Santoro, *Phys. Rev. B* **76**, 144427 (2007).
  - [9] L. E. Sadler *et al.*, *Nature (London)* **443**, 312 (2006).
  - [10] A. Kitaev, *Ann. Phys.* **321**, 2 (2006).
  - [11] A. Kitaev, *Ann. Phys.* **303**, 2 (2003).
  - [12] X.-Y. Feng, G.-M. Zhang, and T. Xiang, *Phys. Rev. Lett.* **98**, 087204 (2007).
  - [13] G. Baskaran, S. Mandal, and R. Shankar, *Phys. Rev. Lett.* **98**, 247201 (2007).
  - [14] H.-D. Chen and Z. Nussinov, arXiv:cond-mat/0703633.
  - [15] D.-H. Lee, G.-M. Zhang, and T. Xiang, arXiv:07053499; K. P. Schmidt, S. Dusuel, and J. Vidal, arXiv:07093017.
  - [16] L.-M. Duan, E. Demler, and M. D. Lukin, *Phys. Rev. Lett.* **91**, 090402 (2003); A. Micheli, G. K. Brennen, and P. Zoller, *Nature Physics* **2**, 341 (2006).
  - [17] See for example, L. Landau and E. M. Lifshitz, *Quantum Mechanics: Non-relativistic Theory*, 2nd Ed. (Pergamon Press, Oxford, 1965); S. Suzuki and M. Okada in *Quantum Annealing and Related Optimization Methods*, Eds. by A. Das and B. K. Chakrabarti (Springer-Verlag, Berlin, 2005).
  - [18] Note that as we approach the gapless phase,  $\Delta E \sim |J_3 - J_{3c}|$  and  $\Delta E \sim |k|$ ; hence  $\nu = z = 1$  for the model [4].
  - [19] E. Altman, E. Demler, and M. D. Lukin, *Phys. Rev. A*

70, 013603 (2004).